AIAA JOURNAL
Vol. 48, No. 8, August 2010

Technical Notes

Control of the Flow over a Delta Wing in the Transonic Regime

Jacques Riou* and Eric Garnier*
ONERA, 92190 Meudon, France
and
Claude Basdevant†
Université Paris 13, 93430 Villetaneuse, France

DOI: 10.2514/1.J050531

Nomenclature

b = half-span of the wing
b_{loc} = local half-span
C_p = pressure coefficient
c = root chord of the wing
c_μ = momentum coefficient
k = fluctuating kinetic energy
ϕ = sweep angle of the wing

I. Introduction

CONTROL of vortical flow over delta wings in the subsonic regime has been the subject of many investigations in recent years. In particular, it has been demonstrated that suction at the leading edge of the wing can improve the aerodynamic performance of the wing [1,2].

However, the capability of such an approach to delay the vortex breakdown occurrence in the transonic regime remains poorly assessed in the literature. Thus, the purpose of this study is to numerically evaluate continuous suction effects on the dynamics of the leading-edge vortex as well as on the aerodynamic performance of the wing in the transonic regime. The considered geometry is the VFE-2 wing used in the RTO-AVT-113 project [3]. The sweep angle ϕ equals 65 deg and the root chord c is equal to 0.4905 m. The freestream Mach number M_∞ equals 0.8, the angle of attack α is set to 25.5 deg and the Reynolds number based on c is $Re_c = 2 \times 10^6$. This study constitutes a follow-up of [4], in which reference computations without control have been validated against experimental data and in which compressibility effects on the vortical flow have been discussed. The vortical flows in subsonic and transonic regimes over the wing have been experimentally investigated at the DLR, German Aerospace Center in Göttingen by Konrath et al. [5–7] and Schröder et al. [8].

The computations are performed using the FLU3M solver [9]. An implicit time integration is employed. The time integration is carried out by means of the second-order-accurate backward scheme of Gear and the time step is set equal to 5×10^{-7} s. The spatial scheme is based on the second-order-accurate AUSM + (P) scheme [10]. The turbulent modeling, based on a coupling of the delayed detached-eddy simulation method [11] with the zonal detached-eddy simulation approach [12] is presented in [13]. The grid is composed of 23×10^6 points. In the vortical flow region, ratio $d_{\text{rans}}/b_{\text{loc}}$ (where d_{rans} is the Reynolds-averaged Navier–Stokes region thickness) does not exceed 0.01. It ensures a large eddy simulation of the whole part of the vortical flow. The averaging process has been performed over a duration of $15T_c$, with T_c being the time scale defined by $T_c = c/U_\infty$. It has been shown in [4] that such a duration allows an accurate prediction of the averaged flow.

Received 4 March 2010; revision received 6 May 2010; accepted for publication 7 May 2010.

*Research Engineer, Applied Aerodynamics Department, 8 rue des Vertugadins.
†Professor, Institut Galilée, 99 Avenue J. B. Clément.

II. Presentation of the Control Strategy

The suction slot is located at the leading edge of the wing, from its apex to $x/c = 0.8$ (see Fig. 1). The latter position is downstream from the location of the vortex breakdown in the reference case. The suction velocity is $U_{\text{slot}} = 170\ \text{m} \cdot \text{s}^{-1}$, which corresponds to a value of the momentum coefficient

$$C_\mu = \frac{\rho_{\text{slot}} S_{\text{slot}} U_{\text{slot}}^2}{0.5 \rho_\infty S_{\text{wing}} U_\infty^2}$$

equal to 2%. In this equation, S_{slot} and S_{wing} are, respectively, the surface of the suction slot and the surface of the wing and ρ_{slot} is the density imposed in the slot.

III. Instantaneous Flow

Figure 2 shows contours of $|\text{grad}(\rho)|$ in a transverse plane at $x/c = 0.5$. As depicted in this figure, the suction applied at the leading edge of the wing deeply alters the flow topology. The crossflow in the reference case is characterized by the formation of five crossflow shocks around the vortical system. In particular, a lambda shock is generated beneath the leading-edge vortex. This shock interacts with the boundary layer, inducing its separation. In the controlled case, this crossflow shock is no longer present and is substituted by an oblique shock sitting on the suction slot. Another fundamental observation is that the secondary vortex does not appear anymore in the suction case. The leading-edge vortex is closer to the wing than in the reference case. The latter feature has also been observed by McCormick and Gursul [1] and Gursul et al. [2] in the subsonic regime.

IV. Suction Effects on the Dynamics of the Vortical Flow

A. Overview of the Crossflow Topology

To characterize the properties of the aforementioned oblique shock sitting on the suction slot, we focus on the flow topology in a plane perpendicular to the leading edge of the wing. Figure 3 shows contours of the normal Mach number M_n and the streamlines in a plane perpendicular to the leading edge of the wing in the suction case. In this figure, b' denotes the local half-span in the new reference frame. Streamlines downstream from the crossflow shock are subjected to two deviations. The first one, θ, occurs right after the shock and can be evaluated as follows:

$$\frac{tg(\sigma - \theta)}{tg(\sigma)} = \frac{\rho_0}{\rho_1} \tag{1}$$

where ρ_0 and ρ_1 are, respectively, the density up- and downstream from the shock and σ is the angle between the shock and the wall. This equation gives a value of θ equal to 17 deg, which is in a reasonable agreement with the value of 15 deg observed in the computation. The second deviation of about 35 deg toward the suction side of the wing is directly induced by the suction. Thus, the

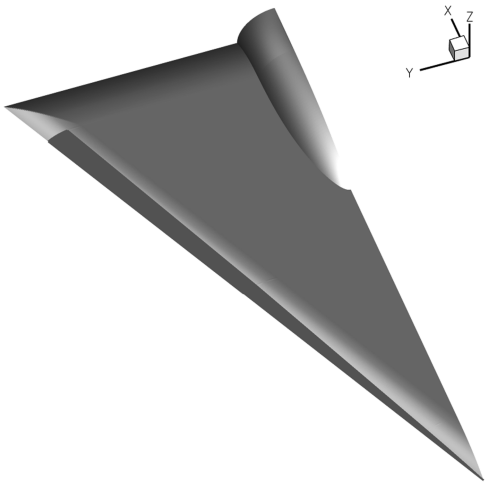

Fig. 1 Representation of the VFE-2 geometry and of the suction slot (dark).

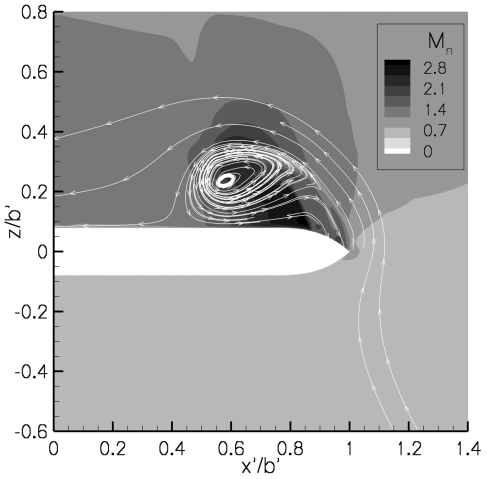

Fig. 3 Contours of the normal Mach number and streamlines in a plane perpendicular to the leading edge of the wing.

crossflow topology in the controlled case highly differs from the one of the reference case. The main modification concerns the displacement of the crossflow shock toward the leading edge of the wing, the suppression of the shock/boundary-layer interaction and of the secondary vortex, and an important deviation of the crossflow toward the wing.

B. Lateral Dynamics of the Vortical Flow

As previously highlighted in [4], in the reference case the crossflow shock beneath the leading-edge vortex is subjected to a lateral unsteadiness which impacts the dynamics of the flow. This phenomenon is illustrated in Fig. 4, showing the probability density function (PDF) of the lateral location of the shock and of the leading-edge vortex core at $x/c = 0.5$. The PDF of the lateral location of the shock presents two sharp peaks in the reference case, illustrating a sinusoidal motion. This motion impacts the dynamics of the leading-edge vortex, as evidenced by the PDF of its lateral core location presenting two large-bands peaks. In the controlled case, the PDF of the lateral location of the shock exhibits a single sharp peak attesting of the suppression of the sinusoidal motion. As a consequence, the leading-edge vortex is stabilized, as testified by the single peak in the PDF of its lateral location. However, it should be noted here that this peak is less acute than that observed in the PDF of the location of the shock, since the vortex is still influenced by the small-scale vortices embedded in the shear layer emanating from the leading edge. This lateral stabilization of the vortex leads to a reduction of the fluctuating kinetic energy, as depicted by Fig. 5 showing the contours of k/U_∞^2 in a plane cutting the vortex core. From the apex of the wing to the vortex breakdown location, levels of k/U_∞^2 are halved in the suction case in comparison with the reference case. Eventually, the vortex breakdown highlighted by a brutal increase of the turbulent kinetic energy occurs. However, this augmentation is less important in the suction case than in the reference case, with the maximal values of k/U_∞^2 being, respectively, equal to 0.38 and 0.5. These results differ from those obtained in the subsonic regime in [1,2], in which an increase of velocity fluctuations in the vortex core when the suction is applied has been observed. It suggests that the decrease of k observed in our study is induced by the suppression of the lateral instability of the vortical flow. One can observe in Fig. 5 that the vortex breakdown is not delayed by the suction, contrary to what is observed in the subsonic regime. The decrease of the swirl level measured in the leading-edge vortex does not delay the vortex breakdown occurrence, since the latter is fixed by a vortex/shock interaction.

V. Suction Effects on the Performance of the Wing

To conclude this study, this section focuses on the suction effects on the aerodynamic performance of the wing. As a starting point, Fig. 6 presents the spanwise distribution of the pressure coefficient C_p as a function of y/b_{loc} for the two cases.

Whatever the location, the intensity of the pressure coefficient peak decreases when the suction is applied. In particular, this decrease reaches 23% at $x/c = 0.2$ and 0.5. At the rear of the suction slot ($x/c = 0.9$), this decrease of C_p is less intense and approximately equals 12%. It results in an increase of the lift coefficient of 22%. Moreover, a decrease of 9% of the drag coefficient is observed. An increase of the performance with suction

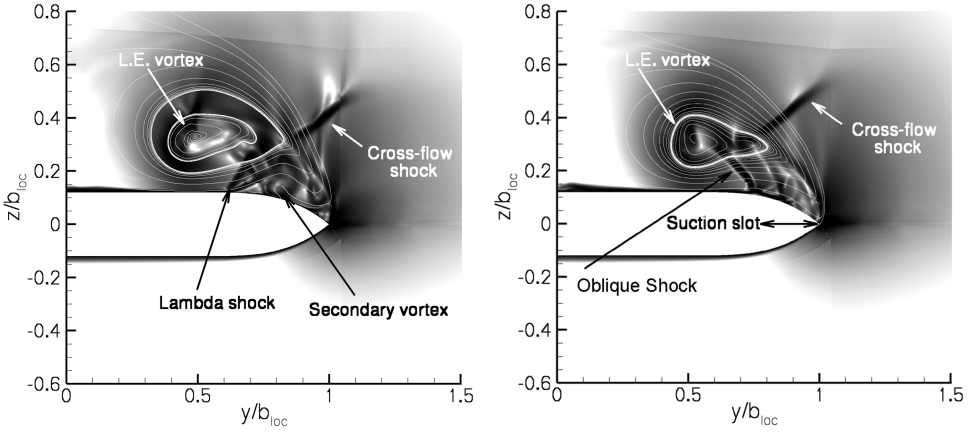

a) b)

Fig. 2 Contours of $|\text{grad}(\rho)|$ at $x/c = 0.5$; reference case (left) and suction case (right).

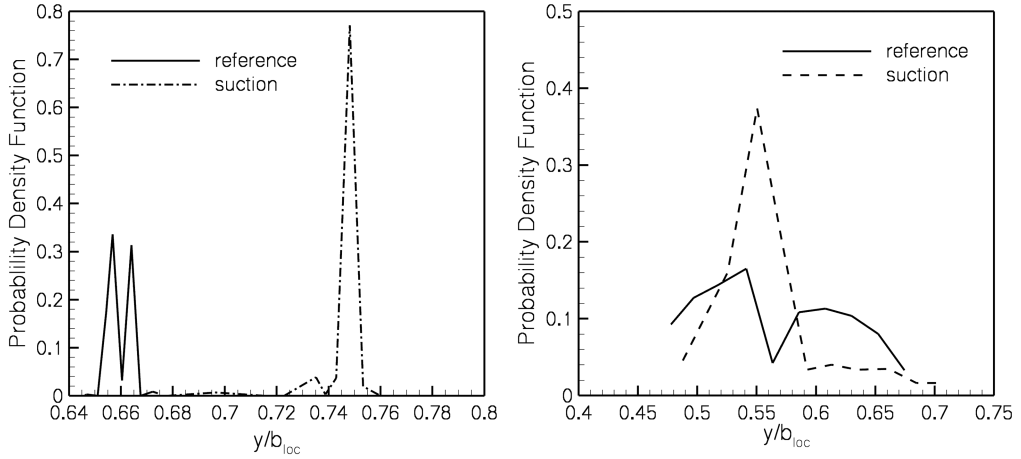

a) b)

Fig. 4 Probability density function of the lateral location of the shock (left) and of the leading-edge vortex core (right).

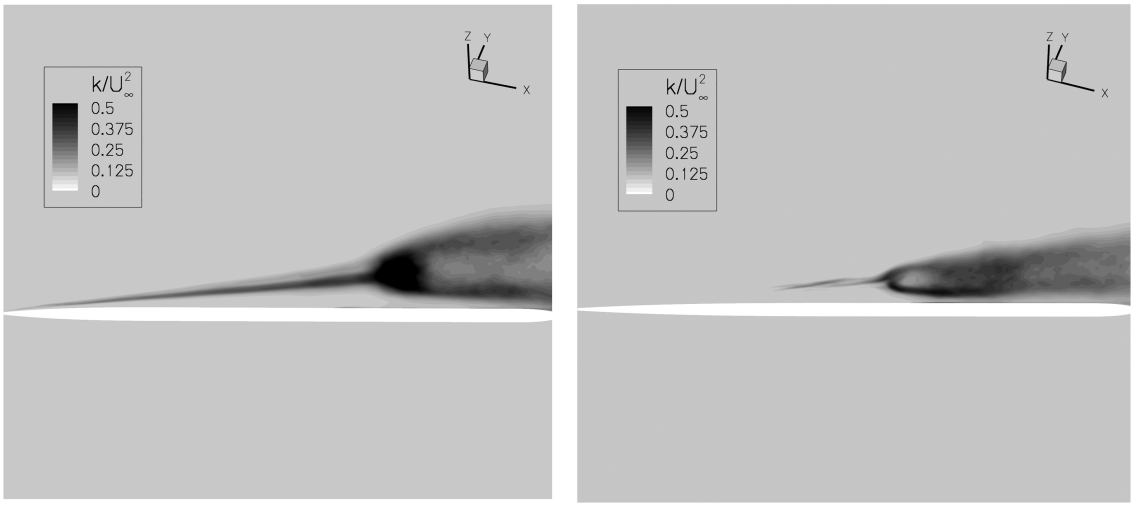

a) b)

Fig. 5 Contours of k/U_∞^2 through the vortex core; reference case (left) and suction case (right).

in the incompressible regime has been experimentally observed but it appears that the involved mechanisms differ. Indeed, following McCormick and Gursul [1] and Gursul et al. [2], in the subsonic regime, the performance enhancement is caused by the delay of the vortex breakdown. In the current study, no delay of breakdown is observed, since this phenomenon is induced by a vortex/shock interaction. The currently observed increase of lift appears to originate from two sources: the displacement of the leading-edge vortex toward the wall and the acceleration of the crossflow induced by the suction.

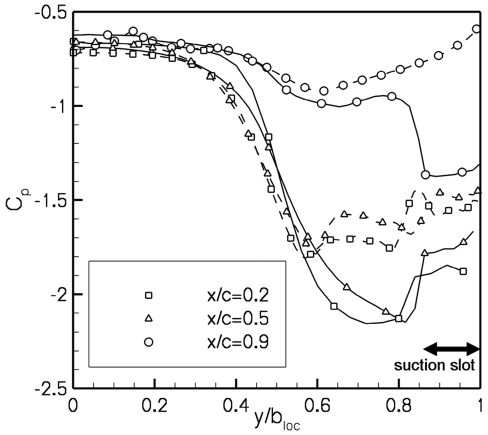

Fig. 6 Spanwise distribution of C_p; reference case (dashed lines) and suction case (solid lines).

VI. Conclusions

Suction effects on the vortical flow over a 65 deg sweep delta wing in the transonic regime have been investigated. The suction slot is located at the leading edge of the wing and the momentum coefficient has been set equal to 2%. It has been shown that suction deeply alters the crossflow topology. In particular, suction moves the leading-edge vortex toward the upper side of the wing and removes both the secondary vortex and the crossflow shock beneath the leading-edge vortex. The latter is replaced by an oblique shock sitting on the slot. It has been demonstrated in the suction case that, contrary to the reference case, this shock is not subjected to a lateral instability. The absence of a lateral instability stabilizes the whole vortical flow and then decreases the fluctuating kinetic energy in the main vortex. As a result, aerodynamic loading fluctuations are decreased by 20%. Moreover, it has been observed that pressure coefficient decreases on the suction side of the wing, increasing its aerodynamic performance.

Acknowledgments

The authors would like to acknowledge the DGA (French Ministry of Defense) for its financial support and would like to thank Robert Konrath of the DLR, German Aerospace Center in Göttingen for having kindly provided the access to the experimental data.

References

[1] McCormick, S., and Gursul, I., "Effect of Shear Layer Control on Leading Edge Vortices," *Journal of Aircraft*, Vol. 33, No. 6, 1996, pp. 1087–1093. doi:10.2514/3.47061

[2] Gursul, I., Wang, Z., and Vardaki, E., "Review of Flow Control Mechanisms of Leading-Edge Vortices," *Progress in Aerospace Sciences*, Vol. 43, No. 7, 2007, pp. 246–270. doi:10.1016/j.paerosci.2007.08.001

[3] Hummel, D., and Redeker, G., "A New Vortex Flow Experiment for Computer Code Validation," NATO, RTO-AVT-113, Loen, Norway, 2001.

[4] Riou, J., Garnier, E., and Basdevant, C., "Compressibility Effects on the Vortical Flow over a 65 Deg Sweep Delta Wing," *Physics of Fluids*, Vol. 22, 2010, Paper 035102. doi:10.1063/1.3327286

[5] Konrath, R., Klein, C., Engler, R. H., and Otter, D., "Analysis of PSP Results Obtained for the VFE-2 65 Deg Delta Wing Configuration at Sub- and Transonic Speeds," AIAA Paper 06-60, Reno, NV, Jan. 2006.

[6] Konrath, R., Schroder, A., and Kompenhans, J., "Analysis Of Piv Results Obtained for the VFE-2 65 Deg Delta Wing Configuration at Sub- and Transonic Speeds," AIAA Paper 06-3003, Reno, NV, Jan. 2006.

[7] Konrath, R., Klein, C., and Schroder, A., "PSP and PIV Investigations on the VFE-2 Configuration in Sub- and Transonic Flow," AIAA Paper 2008-379, Reno, NV, Jan. 2008.

[8] Schröder, A., Agocs, J., Frahnert, H., Otter, D., and Mattner, H., "Application of Stereo PIV to the VFE-2 65 Deg Delta Wing Configuration at Sub- and Transonic Speeds," AIAA Paper 2006-3486, Reno, NV, Jan. 2006.

[9] Pechier, M., Guillen, P., and Cayzac, R., "Magnus Effects over Finned Projectiles," *Journal of Spacecraft and Rockets*, Vol. 38, No. 4, 2001, pp. 542–549. doi:10.2514/2.3714

[10] Mary, I., and Sagaut, P., "Large Eddy Simulation of the Flow Around an Airfoil Near Stall," *AIAA Journal*, Vol. 40, No. 6, 2002, pp. 1139–1146. doi:10.2514/2.1763

[11] Spalart, P. R., Deck, S., Shur, M. L., Squires, K. D., Strelets, M. K., and Travin, A., "A New Version of Detached-Eddy Simulation, Resistant to Ambiguous Grid Densities," *Theoretical and Computational Fluid Dynamics*, Vol. 20, 2006, pp. 181–195. doi:10.1007/s00162-006-0015-0

[12] Deck, S., "Zonal Detached Eddy Simulation of the Flow Around a High Lift Configuration," *AIAA Journal*, Vol. 43, No. 11, 2005, pp. 2372–2384. doi:10.2514/1.16810

[13] Riou, J., Garnier, E., Deck, S., and Basdevant, C., "An Improvement of Delayed Detached Eddy Simulation Applied to a Separated Flow over a Missile Fin," *AIAA Journal*, Vol. 47, No. 2, 2009, pp. 345–360. doi:10.2514/1.37742

P. Tucker
Associate Editor